A Mode MUX/DEMUX for Multicore Fibers With 2D Core Arrays

Junhe Zhou, *Member, IEEE*, and Philippe Gallion, *Senior Member, IEEE*

***Abstract*— In this letter, a mode multiplexer/demultiplexer (MUX/DEMUX) for multicore fibers with 2D aligned cores is proposed. The device is based on the concept of 2D multimode interference (2DMMI) effect. If the 2D waveguide array is aligned within a square lattice, the supermodes of the array will obey the sinusoidal function and coincide with the transfer matrix of the 2DMMI couplers with phase shifter arrays. Therefore, a mode MUX/DEMUX with high mode extinction ratio can be realized based on this principle.**

***Index Terms*— Multimode waveguides, mode division multiplexing.**

I. Introduction

Mode division multiplexing (MDM) has been proposed to further increase the transmission capacity of the fiber communication systems [1]. Apart from the traditional multimode fibers, the multi-core fibers (MCFs), which use different super-modes among the cores to transmit information [2]–[4], can be used in the MDM systems.

Numerous approaches have been proposed to realize the super-mode MUXs/DEMUXs of the MCFs, which are the key components of the MCF-based MDM systems. In [2], free space optics is adopted for mode multiplexing. However, it is quite complex and is difficult to be integrated into the fiber communication systems. An alternative approach is the mode matching method, which is based on the multi-core fiber technology [3] or silicon waveguide technology [4]. The method encounters difficulties while the number of the cores is large, because it requires the cores of the DEMUX to match the propagation constants of the super-modes inside the MCF. Furthermore, if the modes have different spatial distributions but the similar propagation constants, which is usually the case for the MCFs with two dimensionally aligned cores, it is not applicable. The third approach is to use the arrayed waveguide grating (AWG) with phase shifters as a MUX/DEMUX [5]. This ingenious proposal uses the interference inside the AWG to separate different modes of the MCF. This device is compact but suffers the following disadvantages. It is not fiber based and therefore, difficulties arise when it is integrated with the fiber system [3]. Furthermore, the field distribution of the multi-core fiber should obey the sinusoidal function [6] while the AWG fields have equal amplitudes. Hence, the mode extinction ratio will be degraded. Finally, it can not be applied to the MCFs with two dimensionally aligned cores. In summary, for an MCF with a large number of two dimensionally aligned cores, these methods will be either inapplicable or of significant complexity.

MMI couplers [7], [8] have been investigated as mode MUXs/DEMUXs for multimode waveguides [9], [10]. Recently, one dimensional (1D) MMI couplers have been used as MUXs/DEMUXs for the MCFs with equally spaced 1D fiber core arrays [11]. Since 2DMMI couplers can have 2D self-image effect, it is reasonable to use them as the mode MUXs/DEMUXs for the MCFs with two dimensionally aligned cores. In this work, we propose such 2DMMI coupler based mode MUXs/DEMUXs and verify the device functionality via theoretical derivations and numerical simulations. The results of this work differ substantially from those in [11], not only in the extension from 1D to 2D, but also in the novel theory which relates the super-modes in MCFs with two dimensionally aligned cores to the modes in 2DMMI couplers.

Manuscript received January 4, 2014; revised April 11, 2014; accepted May 8, 2014. Date of publication May 16, 2014; date of current version June 13, 2014. This work was supported in part by the National Science Foundation of China under Grant 61201068 and in part by the Fundamental Research Funds for the Central Universities of China.

J. Zhou is with the Department of Electronics Science and Engineering, Tongji University, Shanghai 200092, China (e-mail: jhzhou@tongji.edu.cn).

P. Gallion is with TELECOM ParisTech, Ecole Nationale Supérieure des Télécommunications, Paris 75013, France (e-mail: philippe.gallion@telecom-paristech.fr).

Color versions of one or more of the figures in this letter are available online at http://ieeexplore.ieee.org.

Digital Object Identifier 10.1109/LPT.2014.2323133

II. Mathematical Description

A. Theory for Super-Modes in Two Dimensional Square Waveguide Arrays

MCFs with two dimensionally aligned cores can be viewed as two dimensional waveguide arrays embedded in the infinite cladding. Assuming that a waveguide is the m^{th} waveguide in the x direction and the n^{th} waveguide in the y direction in the two dimensional waveguide array, it will have the amplitude of A_{mn} fulfilling the following coupled mode equation [12]–[13]

$$\begin{aligned} i\frac{dA_{m,n}}{dz} &+ a\left(A_{m+1,n}+A_{m-1,n}\right)+b\left(A_{m,n+1}+A_{m,n-1}\right) \\ &+ c\left(A_{m+1,n+1}+A_{m-1,n-1}\right)+d\left(A_{m+1,n-1}+A_{m-1,n+1}\right)=0 \end{aligned} \tag{1}$$

where a and b are the coupling constants in the x direction and the y direction, and c and d the coupling constants in the diagonal directions [12]. For a square array, the contribution from diagonal coupling can be neglected and therefore c and d can be set to be 0 in Eq. (1), and $a = b$ [12]. Hence Eq. (1)

can be decomposed into two coupled equations [12]

$$
\begin{aligned}
i\frac{dB_{m,n}}{dz} + a\left(B_{m+1,n} + B_{m-1,n}\right) &= 0 \\
i\frac{dC_{m,n}}{dz} + a\left(C_{m+1,n} + C_{m-1,n}\right) &= 0 \\
A_{m,n} &= B_{m,n}C_{m,n}
\end{aligned} \tag{2}
$$

The two equations in Eq. (2) are actually the coupled equations for the 1D arrays in the x direction and the y direction, and the expressions for the super-modes can be derived [6]. Therefore, in the two dimensional square lattice, the super-modes will be

$$\phi_{p,q}(m,n) = \sin\left(\frac{mp\pi}{N}\right)\sin\left(\frac{nq\pi}{N}\right) \tag{3}$$

where $N - 1$ is the number of the waveguides within one dimension and the total number of waveguides is $(N-1)^2$, p and q the super-mode orders in the x direction and the y direction.

B. Theory of Two Dimensional MMI Coupler

The input/output fields of the 2DMMI coupler can be formulated by [14]

$$\mathbf{A_{out}} = \mathbf{M_v A_{in} M_u} \tag{4}$$

where $\mathbf{A_{in}}$ is the input matrix, $\mathbf{A_{out}}$ the output matrix, $\mathbf{M_u}$ and $\mathbf{M_v}$ the transfer matrixes in the x direction and the y direction, which can be calculated by [14]

$$
\begin{aligned}
\mathbf{M_v} &= \mathbf{V B_v V^T} \\
\mathbf{M_u} &= \mathbf{U^T B_u U}
\end{aligned} \tag{5}
$$

where $\mathbf{U}$ and $\mathbf{V}$ are orthogonal matrixes relating the input field to the propagation modes in the x direction and the y direction, $\mathbf{B_u}$ and $\mathbf{B_v}$ the matrixes indicating the phase change induced by the internal modal propagation.

For 2DMMI couplers with a square shape, the length of the two dimensional MMI coupler is set to be [8], [14]

$$L_N = \frac{2nW_e^2}{N\lambda_0} \tag{6}$$

where n_{eff} is the effective index of the fundamental mode of the MMI coupler, λ_0 the free space wavelength, W_e the effective width/height of the MMI coupler. Hence, the diagonal elements of the matrixes $\mathbf{B_u}$ and $\mathbf{B_v}$ can be evaluated as [8]

$$
\begin{aligned}
b_{v,ii} &= \exp\left(j\frac{i^2\pi}{2N}\right) \\
b_{u,ii} &= \exp\left(j\frac{i^2\pi}{2N}\right)
\end{aligned} \tag{7}
$$

If the input and output ports are placed at the position of [8]

$$
\begin{aligned}
x_i &= \frac{iW_e}{N} = iD \quad (i = 1 \ldots N-1) \\
y_i &= \frac{iW_e}{N} = iD \quad (i = 1 \ldots N-1)
\end{aligned} \tag{8}
$$

the orthogonal matrixes $\mathbf{U}$ and $\mathbf{V}$ will have the elements as [8]

$$U_{ik}/V_{ik} = \sqrt{\frac{2}{N}}\sin\left(\frac{ik\pi}{N}\right) \quad (i,k = 1 \ldots N-1) \tag{9}$$

After some lengthy derivations, the elements of $\mathbf{M_u}$ and $\mathbf{M_v}$ can be derived analytically as [8], [14]

$$M_{u/v}(l,k) = j\exp\left(j\frac{\pi}{4}\right)\sqrt{\frac{2}{N}}\exp\left(-j\frac{(l^2+k^2)\pi}{2N}\right)\sin\left(\frac{lk\pi}{N}\right) \tag{10}$$

C. Two Dimensional MMI Coupler as a Mode MUX/DEMUX

If the constant term in Eq. (11) is ignored, it can be seen that the elements of the transfer matrixes $\mathbf{M_u}$ and $\mathbf{M_v}$ fulfill the sinusoidal function with some phase deviations. The phase deviations can be eliminated by adding phase shifters at the input/output ports. If phase shifters with the phase shift of $(l^2 + k^2)\pi/2N$ are placed at the input and output ports, the transfer matrix $\mathbf{M_u}$ and $\mathbf{M_v}$ will be modified to $\mathbf{T_u}$ and $\mathbf{T_v}$ as [14]

$$
\begin{aligned}
\mathbf{T_V} &= \mathbf{D_{x,out} M_V D_{x,in}} \\
\mathbf{T_U} &= \mathbf{D_{y,in} M_U D_{y,out}}
\end{aligned} \tag{11}
$$

The elements of $\mathbf{T_u}$ and $\mathbf{T_v}$ will be

$$T_{u/v}(l,k) = j\exp\left(j\frac{\pi}{4}\right)\sqrt{\frac{2}{N}}\sin\left(\frac{lk\pi}{N}\right) \tag{12}$$

It can be seen that the expression in Eq. (12) coincides with the sinusoidal function. If an optical field has the input matrix $\mathbf{A_{in}}$ with the elements as Eq. (3)

$$A_{in}(m,n) = \sin\left(\frac{mp\pi}{N}\right)\sin\left(\frac{nq\pi}{N}\right) \tag{13}$$

since $\mathbf{A_{out}} = \mathbf{T_v A_{in} T_u}$, there will be an output optical wave at the output port of p, q and no optical waves at other ports. In this way, the mode MUX/DEMUX can be realized.

It should be noted that although the phase shifters are added at the input and the output ports in the above analysis to ease the mathematical formulation, it is not necessary to have them at the output ports during real applications, because they will not impact the mode discrimination process.

III. Numerical Results and Discussion

In order to verify the theoretical predictions, numerical simulations based on the three dimensional beam propagation method (3DBPM) has been carried out on a 3 × 3 port mode MUX/DEMUX. The MCF discussed in this letter uses similar materials and structures in [3]–[5] and our previous work [11]. For readers' convenience, we restate here as follows. The cladding index is 1.45 and the core index is 1.4674. The diameters of the cores are 5μm. The nine cores of the two dimensional MCF are aligned within a 3 × 3 square lattice with the spacing between the adjacent cores to be D. A rectangle core fiber, which has the same core and cladding index, is used as the MMI device. The effective width and the

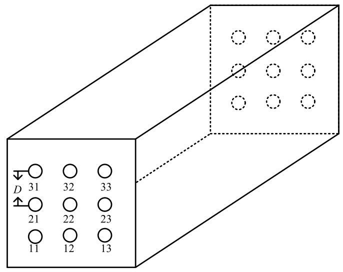

Fig. 1. Schematic of the 2DMMI coupler based MUX/DEMUX with port labeling.

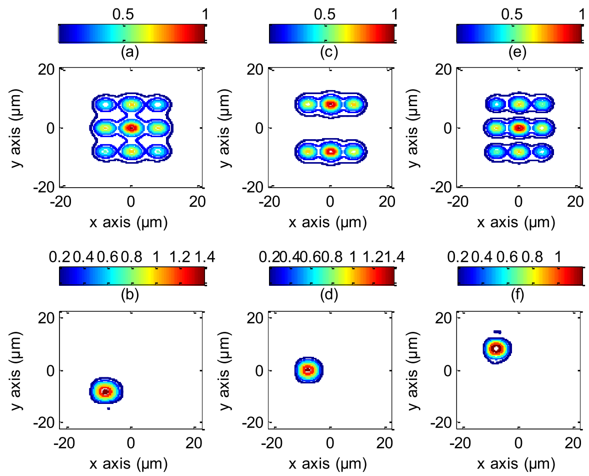

Fig. 2. The normalized super-modes of the MCF and the fields at the output of the DEMUX with $D = 8\mu$m: (a) mode 11, (b) the field at the output of the DEMUX for mode 11, (c) mode 12, (d) the field at the output of the DEMUX for mode 12, (e) mode 13, (f) the field at the output of the DEMUX for mode 13.

effective height of the rectangle core fiber are both $4D$. The length of the rectangle core fiber can be calculated by Eq. (6) and should be adjusted slightly according to the simulations. The schematic of the device with port labeling is illustrated in Fig. 1.

There are several approaches to realize the phase shifters before the input ports of the device, including using arrayed waveguides with different lengths [5] or different refractive indexes [3], or using external phase shifters [15]. In the simulation, a perfect external phase shifter array is assumed.

Firstly, we assume the distance between the cores, i.e. D, to be 8μm and examine the super-modes de-multiplexing capability. The signal wavelength is 1550nm. The effective width and height of the MMI device are 32μm, while the length is 504μm. During the simulation, the step size is 0.1μm in the x direction and the y direction, and 1μm in the z direction. All the modal fields have been normalized with the peak value of 1. In Fig. 2–4, total nine modes of the 3×3 two dimensional MCF, from mode 11 to mode 33, are used as the input to the DEMUX. As illustrated, the output waves concentrate on the corresponding output ports. For instance, if mode 33 is injected into the device (fig. 4 (e)), the wave will appear at the output port 33 (fig. 4(f)). These figures clearly demonstrate that the device has distinguished different modes of the MCF successfully. The mode extinction ratio, which is defined as the power at the corresponding output port over the powers at other output ports, is around 26dB.

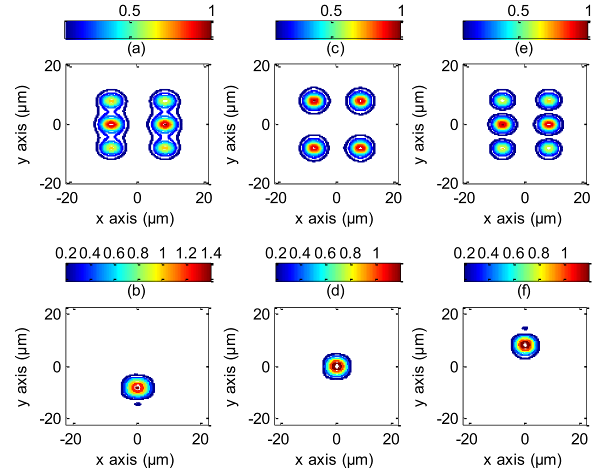

Fig. 3. The normalized super-modes of the MCF and the fields at the output of the DEMUX with $D = 8\mu$m: (a) mode 21, (b) the field at the output of the DEMUX for mode 21, (c) mode 22, (d) the field at the output of the DEMUX for mode 22, (e) mode 23, (f) the field at the output of the DEMUX for mode 23.

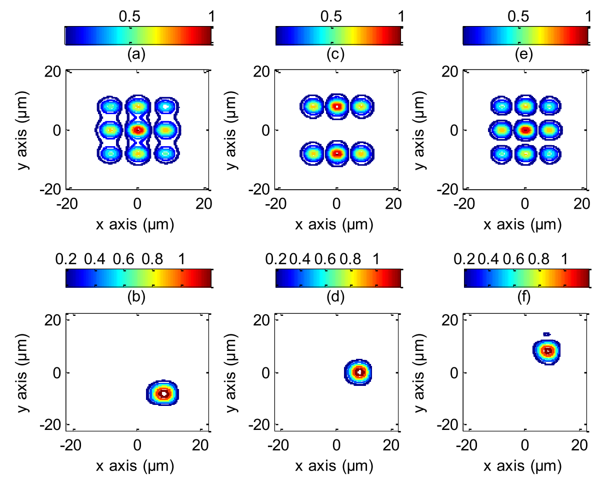

Fig. 4. The normalized super-modes of the MCF and the fields at the output of the DEMUX with $D = 8\mu$m: (a) mode 31, (b) the field at the output of the DEMUX for mode 31, (c) mode 32, (d) the field at the output of the DEMUX for mode 32, (e) mode 33, (f) the field at the output of the DEMUX for mode 33.

To further illustrate the device as a DEMUX, two modes, i.e. mode 11 and mode 33, are combined with the same phase and the power ratio of 1:1. It is injected into the device (fig. 5(a)), and at the output of the device, the two modes are clearly de-multiplexed with the correct amplitudes (fig. 5(f)). The fields during the propagation inside the device are illustrated in Fig. 5(b-e) demonstrating the transformation process.

The device can not only be used as a DEMUX, but also as a MUX or a mode generator. As shown in Fig. 6, if the device is used inversely with the input fields concentrating on port 11, port 12 and port 22, the super-modes of the MCF can be generated. To compare with the ideal modes in Fig. 2–4, the correlation coefficients based on the normalized overlap integral are calculated as 0.95, 0.96, and 0.97 for the three pairs of modes, showing excellent modal matching between them.

The robustness of the device is investigated while changing the distance between the cores. The smaller D is, the stronger

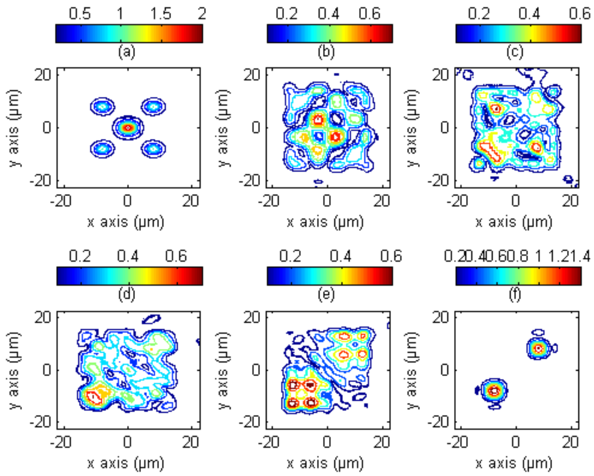

Fig. 5. The combination of super-modes of the MCF and the fields at the output of the DEMUX: (a) the combination of mode 11 and mode 33 with the same phase and the power ratio of 1:1, (b) the field along the structure length at 100 μm, (c) the field along the structure length at 200 μm, (d) the field along the structure length at 300 μm, (e) the field along the structure length at 400 μm, (f) the field at the output of the DEMUX.

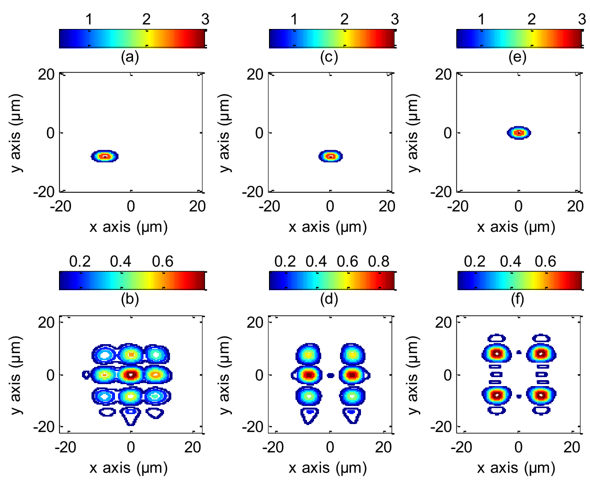

Fig. 6. The mode MUX/DEMUX functions as a mode generator: (a) the input field at port 11, (b) the field of the generated mode 11 at the output of the device, (c) the input field at port 21, (d) the field of the generated mode 21 at the output of the device, (e) the input field at port 22, (f) the field of the generated mode 22 at the output of the device.

the coupling between the cores is, which might impact the performance of the device. In the simulations, D is varied with the value of 7μm and 10μm while the length of the MMI couplers varies accordingly. The mode extinction ratios are close to 26dB for both cases. Hence, the distance between the cores will not impact the performance. Furthermore, no wavelength dependency on D is found in the simulations.

Finally, the fabrication error tolerance of the device is studied. We use the case with $D = 8\mu$m as an example. When the length has about 25μm error, which is about 5% of the total length, the mode extinction ratio degrades to 20dB. When the width has about 1μm error, which is about 3% of the total width, the mode extinction ratio degrades to 20dB. This is in agreement with the analysis in [16], which indicated that the width error has a stronger impact on the MMI coupler performance and it can be proportionally related to the length error by a factor of 2 [16]. The operation wavelength range can be evaluated by relating the wavelength deviation to the length deviation [16]. Another type of error, which arises from the inaccuracy of the phase shifters, is also investigated. When the phase shifters have 5% phase error for each phase shifter, the mode extinction ratio degrades to about 22dB. Therefore, the device is quite robust with respect to the fabrication inaccuracies. However, in order to keep a better performance, the length/width of the device should be accurately fabricated/adjusted. Also, the phase shifters should be adjusted to provide a precise phase shift.

IV. Conclusion

In summary, we have proposed a novel mode MUX/DEMUX for a MCF, whose cores are aligned in a two dimensional square lattice. Detailed theoretical derivations and numerical verifications are provided. The proposed device shows a robust performance with a high mode extinction ratio. The device can be fiber-based and is easy to be integrated into the fiber communication system.

References

[1] H. R. Stuart, “Dispersive multiplexing in multimode optical fiber,” *Science*, vol. 289, no. 5477, pp. 281–283, 2000.

[2] R. Ryf *et al.*, “Coherent 1200-km 6 × 6 MIMO mode-multiplexed transmission over 3-core microstructured fiber,” in *Proc. ECOC*, Sep. 2011, paper Th.13.C.1.

[3] F. Saitoh, K. Saitoh, and M. Koshiba, “A design method of a fiber-based mode multi/demultiplexer for mode-division multiplexing,” *Opt. Exp.*, vol. 18, no. 5, pp. 4709–4716, 2010.

[4] L.-W. Luo *et al.*, “WDM-compatible mode-division multiplexing on a silicon chip,” *Nature Commun.*, vol. 5, pp. 1–7, Jan. 2014.

[5] Y. Kokubun and M. Koshiba, “Novel multi-core fibers for mode division multiplexing: Proposal and design principle,” *IEICE Electron. Exp.*, vol. 6, no. 8, pp. 522–528, 2009.

[6] E. Kapon, J. Katz, and A. Yariv, “Supermode analysis of phase-locked arrays of semiconductor lasers,” *Opt. Lett.*, vol. 9, no. 4, pp. 125–127, 1984.

[7] S.-Y. Tseng, Y. Kim, C. J. Richardson, and J. Goldhar, “Implementation of discrete unitary transformations by multimode waveguide holograms,” *Appl. Opt.*, vol. 45, no. 20, pp. 4864–4872, 2006.

[8] J. M. Heaton and R. M. Jenkins, “General matrix theory of self-imaging in multimode interference (MMI) couplers,” *IEEE Photon. Technol. Lett.*, vol. 11, no. 2, pp. 212–214, Feb. 1999.

[9] J. B. Park, D.-M. Yeo, and S.-Y. Shin, “Variable optical mode generator in a multimode waveguide,” *IEEE Photon. Technol. Lett.*, vol. 18, no. 20, pp. 2084–2086, Oct. 15, 2006.

[10] A. L. Y. Low, Y. S. Yong, A. H. You, S. F. Chien, and C. F. Teo, “A five-order mode converter for multimode waveguide,” *IEEE Photon. Technol. Lett.*, vol. 16, no. 7, pp. 1673–1675, Jul. 2004.

[11] J. Zhou and P. Gallion, “A novel mode multiplexer/demultiplexer for multi-core fibers,” *IEEE Photon. Technol. Lett.*, vol. 25, no. 13, pp. 1214–1217, Jul. 1, 2013.

[12] A. Szameit, T. Pertsch, F. Dreisow, S. Nolte, and A. Tünnermann, “Light evolution in arbitrary two-dimensional waveguide arrays,” *Phys. Rev. A*, vol. 75, no. 5, pp. 053814-1–053814-14, 2007.

[13] T. Pertsch *et al.*, “Discrete diffraction in two-dimensional arrays of coupled waveguides in silica,” *Opt. Lett.*, vol. 29, no. 5, pp. 468–470, 2004.

[14] J. Zhou, “Two-dimensional discrete sine transform and discrete cosine transform based on two-dimensional multimode interference couplers,” *IEEE Photon. Technol. Lett.*, vol. 22, no. 21, pp. 1613–1615, Nov. 1, 2010.

[15] X. Yang *et al.*, “Primary experiments on 2-D and 1-D fiber-type optical phased array,” *Proc. SPIE*, vol. 7136, p. 71363J, Nov. 2008.

[16] A. R. Gupta, K. Tsutsumi, and J. Nakayama, “Synthesis of Hadamard transformers by use of multimode interference optical waveguides,” *Appl. Opt.*, vol. 42, no. 15, pp. 2730–2738, 2003.